J. COMBIN. MATH. COMBIN. COMPUT. 127b (2025) 1307--1325

Journal of Combinatorial Mathematics
and Combinatorial Computing
www.combinatorialpress.com/jcmcc

Combinatorial Press

Prediction and Anomaly Detection of Coal Mill Outlet Pressure Using a PSO-3DResNet Model

Shiguang Guo[1,✉]

[1] *Beijing Information Science and Technology University, Beijing, 100025, China*

ABSTRACT

This paper improves the deep residual network, proposes 3DResNet network and carries out particle swarm optimization, constitutes the PSO-3DResNet model, and designs the coal mill fault diagnosis model based on PSO-3DResNet model. The technical parameters, common fault types and fault characteristics of the coal mill are analyzed, and the relationship between the input and output parameters of the coal mill is decomposed by the residual-based condition monitoring method. Combining the numerical simulation model of coal mill and historical operation data, the typical fault condition monitoring of coal mill is constructed. Compare the classification accuracy of each model on the working state of blast furnace wind mouth, and get the anomaly detection performance of each model. The PSO-3DResNet model is analyzed to monitor the normal operating state of the coal mill, and the model is tested using the historical current and outlet wind temperature anomaly data of the coal mill. When the coal mill is in an abnormal state, the estimated residuals of the current abnormal condition fluctuate within [-16,3] with a small range, and the weighted average residuals of the current abnormal condition index remain within [-4,1].

Keywords: PSO; 3DResNet model; anomaly detection; typical fault detection; coal mill

1. Introduction

Coal mill is an important equipment in coal-fired power plant, and its main function is to grind coal powder into fine powder for combustion. And the air volume and outlet pressure of the coal mill are two important parameters for the normal operation of the coal mill, and the relationship between them will directly affect the working efficiency and safety performance of the coal mill [1-4]. The coal mill will introduce the flue gas through the induced draft fan to form a certain air volume and discharge it through the outlet. When the air volume gradually increases, a certain outlet pressure will be formed. Therefore, there is a certain positive correlation between the air volume and outlet pressure of the coal mill [5-8]. However, in actual operation, the factors affecting the air volume and outlet pressure

✉ Corresponding author.
E-mail address: beiergo@yahoo.com (S. Guo).
Received 05 March 2024; Revised 20 June 2024; Accepted 15 November 2024; Published Online 16 April 2025.
DOI: 10.61091/jcmcc127b-072
© 2025 The Author(s). Published by Combinatorial Press. This is an open access article under the CC BY license (https://creativecommons.org/licenses/by/4.0/).

are more complicated. For example, the inlet air temperature, inlet air humidity, coal powder particle size, mill deflection angle, etc. will have a certain impact on the air volume and outlet pressure [9-11].

As for China, coal energy has long been in the dominant position among all energy sources, and it is an important industry to maintain the national economic level and energy production [12-13]. However, the frequent occurrence of disasters due to abnormal coal mill outlet pressure of coal mills has brought great influence to the safe production of coal mines and serious risk to the personal safety of workers [14-16]. Therefore, coal mill outlet pressure prediction and anomaly detection are of great significance to ensure the safety of personnel and property, and the PSO-3DResNet model can play an important role in this pressure prediction and anomaly detection [17-19].

This paper decomposes the PSO-3DResNet model composition, establishes the coal mill operation state monitoring model by using the PSO-3DResNet model, and derives the PSO-3DResNet model fault diagnosis steps. Analyze the main technical parameters of the coal mill and construct a numerical simulation model of the coal mill. Combine the structured and unstructured grids in the grid setting, set the primary duct inlet as the mass inlet boundary condition, and numerically simulate the two types of coal mills respectively. The common fault types of coal mills are listed, and the typical fault condition monitoring of coal mills is established based on the residual condition monitoring method. The PSO-3DResNet model proposed in this paper is utilized to decompose each parameter of the normal state of the coal mill. Combine the deviation values of observed and estimated values to analyze the operating status of the coal mill.

2. PSO-3D ResNet model

2.1. Deep residual networks (ResNet)

The ResNet model is essentially an upgraded version of the ConvNet model, which is the core methodology used in this paper for coal mill outlet fault diagnosis. It usually consists of a combination of important basic modules such as an input layer, a series of convolutional layers, batch normalization, constant mapping, global mean pooling, and a fully connected output layer [20-21].

1) The convolutional layer can be considered as one of the core parts of the ConvNet model as well as the ResNet model. The convolutional layer adopts both local sensing and weight sharing to reduce the scale of parameters that need to be trained inside the deep neural network, which effectively reduces the training difficulty of deep neural networks. In general, the operation of 2D convolution can be expressed as:

$$\begin{aligned} Y_{Conv}\left(i_{ro},i_{co},j_{ch}\right) = \sum_{j_{ro}}\sum_{j_{co}}\sum_{i_{ch}}\Big(& X_{Conv}\left(i_{ro}-j_{ro},i_{co}-j_{co},i_{ch}\right) \\ & \cdot P_{\ker}\left(j_{ro},j_{co},i_{ch},j_{ch}\right)+P_{blas}\left(j_{ch}\right)\Big) \end{aligned} \tag{1}$$

where X_{Conv} denotes the input feature map of the convolutional layer. $P_{\ker}$ denotes the weight parameters in the convolution kernel, P_{blas} denotes the bias parameters, and Y_{Conv} denotes the corresponding output feature map. In general, the parameters contained in $P_{\ker}$ and P_{blas} need to be trained using the error back propagation algorithm. i_{ro}, i_{co} and i_{ch} denote the indexes of rows, columns and channels in X_{Conv}, respectively. i_{ch} is also used to denote the index of the channel in $P_{\ker}$. j_{ro} and j_{co} denote the indexes of rows and columns in $P_{\ker}$, respectively. j_d denotes the index of channel in Y_{Conv}.

Meanwhile, the size of the convolutional kernel in the ResNet model in this paper is set to 3×3. Compared with the convolutional kernel of size 5×5 or larger, the convolutional kernel of size 3×3 has a lower computing power.

2) In this paper, the Tanh activation function is used, and the Tanh activation function can be expressed as:

$$y_{\tanh} = \frac{e^{x_{\tanh}} - e^{x_{\tanh}}}{e^{x_{\tanh}} + e^{x_{\tanh}}} \tag{2}$$

where $x_{\tanh}$ and $y_{\tanh}$ denote the input and output of the Tanh activation function, respectively. It can be seen that $y_{\tanh}$ takes values in the interval between -1 and 1.

The partial derivatives of the Tanh activation function take values in the interval between zero and one. Similar to the Sigmoid activation function, as the absolute value of x increases, its partial derivative gradually tends to zero. The formula for its partial derivative can be expressed as:

$$\frac{\partial y_{\tanh}}{\partial x_{\tanh}} = 1 - \left(y_{\tanh}\right)^2 \tag{3}$$

In recent years, the ReLU activation function has been widely used in deep learning algorithms, and it works by outputting negative features as zero, which can be expressed as:

$$y_{\mathrm{Re}LU} = \begin{cases} x_{\mathrm{Re}LU} & if\ x_{\mathrm{Re}LU} > 0 \\ 0 & if\ x_{\mathrm{Re}LU} \le 0 \end{cases} \tag{4}$$

where x_{ReLU} and y_{ReLU} are the input and output features of the ReLU activation function, respectively.

The partial derivatives of the ReLU activation function can take the value of zero or one only and can be expressed in the form of Eq:

$$\frac{\partial y_{\mathrm{Re}LU}}{\partial x_{RCLU}} = \begin{cases} 1 & if\ x_{\mathrm{Re}LU} > 0 \\ 0 & if\ x_{\mathrm{Re}L.U} < 0 \end{cases} \tag{5}$$

3) Batch normalization is a normalization method proposed for this internal covariance drift problem. Different from the general normalization method, batch normalization is an operation embedded between layers within the deep neural network, which can be expressed as:

$$\mu = \frac{1}{N_{batch}} \sum_{s=1}^{N_{batch}} x_s \tag{6}$$

$$\sigma^2 = \frac{1}{N_{batch}} \sum_{s=1}^{N_{batch}} \left(x_s - \mu\right)^2 \tag{7}$$

$$z_s = \frac{x_s - \mu}{\sqrt{\sigma^2 + \varepsilon}} \tag{8}$$

$$y_s = \gamma z_s + \beta \tag{9}$$

where x_s refers to some one-dimensional feature of the s nd sample in a batch. N_{batch} refers to the number of samples included in each batch, ε is a constant very close to zero, and y_s is the output feature corresponding to x_s. The optimization process for γ and β is implemented using gradient descent and can be expressed as:

$$\gamma \leftarrow \gamma - \frac{\eta}{N_{batch}} \sum_s \sum_k \frac{\partial E_s}{\partial Path\_r_k} \frac{\partial Path\_r_k}{\partial \gamma} \tag{10}$$

$$\beta \leftarrow \beta - \frac{\eta}{N_{batch}} \sum_s \sum_k \frac{\partial E_s}{\partial Path\_b_k} \frac{\partial Path\_b_k}{\partial \beta} \tag{11}$$

where η refers to the learning rate, which is often a decimal number less than 1 and greater than 0. E_s is the cross-entropy error for the s rd sample. $Path\_r$ and $Path\_b$ denote the set of all differentiable paths used to represent the connections γ and β with the cross-entropy error, respectively.

4) ResNet models usually contain a certain number of basic residual modules, and these basic residual modules are the core components of ResNet models. The basic residual module ReLU activation functions are all in a path on one side of it. The operations contained in this path are "batch normalization → ReLU activation function → convolutional layer → batch normalization → ReLU activation function → convolutional layer".

5) The ResNet model used in this paper adopts the global mean pooling operation near the output layer. Global mean pooling refers to calculating its corresponding mean value as the output feature from the feature map of each channel separately, which can be expressed as:

$$Y_{GAP}\left(1,1,i_{ch}\right)=\underset{i_{ro},i_{co}}{average}\left(X_{GAP}\left(i_{ro},i_{co},i_{ch}\right)\right) \tag{12}$$

where X_{GAP} and Y_{GAP} denote the input feature map and output feature map of global mean pooling, respectively.

6) The cross-entropy loss function is a classical loss function that is often used in the multi-classification problem of neural networks. In the ResNet model, the feature dimension of the output layer is the same as the number of classes involved in training. Before calculating the cross-entropy loss function, it is first necessary to use the oftmax function to force the features x_j, $j=1,2,\ldots,N_{class}$ of the output layer to be transformed into decimals in the interval $\left[0,1\right]$. Where N_{class} denotes the number of categories involved in this classification task. Softmax function can be expressed in the form of Eq:

$$y_j=\frac{e^{x_j}}{\sum_{i=1}^{N_{class}}e^{x_i}} \tag{13}$$

The cross-entropy loss function can be defined as:

$$L=-\sum_{j=1}^{N_{class}}t_j\log y_j \tag{14}$$

Where t_j represents the true label of the sample and y_j represents the output of the softmax function. In general, the cross-entropy loss function leads to higher training speeds in neural network-based multi-classification problems compared to the more traditional squared error function.

2.2. 3D ResNet Network Architecture

2.2.1. 3D Convolution. The input data of traditional 2D convolution is a single-frame image, and the internal core is the 2D convolution kernel $\left(i\times i\right)$. Since the convolution calculation of 2D convolution involves only the spatial dimension, i.e., the height and width of a single-frame image are used as the dimensions for the calculation, the problem to be processed cannot be accurately categorized due to the loss of timing information to a large extent. In 3D convolution, the input data are multiple consecutive frames of images. In the calculation, 3D convolution improves the convolution kernel of 2D convolution from $i\times i$ to $i\times i\times i$, which is the essential difference between 3D convolution and 2D convolution. Multiple consecutive video frames are computed through the 3D convolutional layer in chronological order, i.e., the motion feature information with temporal order is obtained. The whole calculation process is shown in equation (15):

$$v_{i,j}^{x,y,t}=f\left(\sum_{k=1}^{m}\sum_{p=1}^{P_i}\sum_{q=1}^{Q_i}\sum_{r=1}^{R_i}w_{i,j,k}^{(p,\cdot,r}v_{i-1,k}^{x+p,y+q,i+r}+b_{i,j}\right) \tag{15}$$

where $v_{i,j}^{x,y,t}$ denotes the eigenvalue at the j rd output feature map (x,y,t) of layer i. m denotes the number of feature maps in the previous layer, i.e., the number of channels in the previous layer. P_i, Q_i, and R_i denote the height dimension, width dimension, and time dimension of the 3D convolution kernel of layer i, respectively. $w_{i,j,k}^{p \cdot q \cdot r}$ denotes the size of the convolution kernel corresponding to the k th feature map of the $(i-1)$ th layer. $b_{i,j}$ denotes the bias value of the j th channel of layer i, and f denotes the activation function.

2.2.2. 3D ResNet Network. The internal convolution kernel of the 3D Res Net network uses 3D convolution, and its network structure is similar to that of the 2D Res Net network. The network structure is similar to the 2D Res Net network. It consists of one base module Layer, and these Layers contain a number of residual blocks. The residual blocks are classified into two categories according to their structure: Ba-sic Block and Bottleneck. The core of the residual blocks is the residual structure, i.e., a Skip-Layer is added every few layers of convolution. On top of the sequential connection of each layer of a traditional neural network, the Skip-Layer connects the top of the residual block to the network layer before the last Re LU activation function in the block. That is, the input data not only passes through the network sequentially, but also undergoes a skip connection.

The 3D Res Net-18 and 3D Res Net-34 networks use a Ba-sic Block residual block. The Basic Block consists of two 3 × 3 × 3 convolutional layers, each followed by a batch normalized BN layer and a Re LU activation function layer. To deepen the network to handle more complex problems, another type of residual block-Bottleneck is used.

2.3. Particle Swarm Optimization-based Fault Diagnosis for 3DResNet

2.3.1. Particle Swarm Optimization Algorithm. The basic idea of the particle swarm algorithm is that each potential solution to the optimization problem is a particle in the search space, and all particles have a fitness value determined by the function being optimized. Each particle also has a velocity vector that determines the direction and distance in which they fly, and the particles then follow the current optimal particle in the search of the solution space. The particle swarm optimization algorithm first initializes a group of random particles and uses multiple iterations to search for the optimal solution [22].

In each iteration, a particle updates itself by tracking two poles, the individual pole p_{best} and the global pole g_{best}. The individual pole is the optimal position that a single particle passes through, and the global pole is the optimal position among the optimal positions that all the particles in the individual particle swarm pass through. The particles update their velocity and position according to the individual and global extreme values. In finding these two optimal values, the particle updates its velocity and position according to Eqs. (16) and (17):

$$\begin{aligned} v = \omega \times v + C_1 \times Rand() \times \left(p_{best} - x\right) \\ + C_2 \times Rand() \times \left(g_{best} - x\right) \end{aligned} \tag{16}$$

$$x = x + v \tag{17}$$

Where, v is the velocity of the particle, x is the current position of the particle. $Rand(\ )$ is a random number between (0, 1), p_{best} is the individual extreme value. g_{best} is the global extreme value, C_1, C_2 are the learning factors.

2.3.2. Troubleshooting steps. In this section, Matlab 7.6 will be used as the development environment to diagnose the fault data of the powder making system based on the particle swarm optimization 3DResNet toolbox.

In this paper, particle swarm optimization algorithm is used to achieve the optimization of 3DResNet

parameters.The steps of PSO-3DResNet diagnosis section are described as follows:
1) The data preprocessing stage normalizes the training and test data and removes redundant data using the Marginal Distance Construct D matrix, which is handled in the same way as data preprocessing in fault diagnosis.
2) Initialization, by Eq. (16), defines the particle space dimension as 2, and the particle position values are determined by the support vector machine parameters γ and σ^2. Set $\left(\gamma,\sigma^2\right)$ range as $\{0.05,1000;0.001,200\}$, ω search interval as $[0.8,1.2]$. ν search interval as $[0.5,2]$, acceleration constant $C_1=2$, $C_2=2$. Maximum number of iterations $T_{\max}=100$, population size $m=40$.
3) The adaptation value F is the deep residual network fault diagnosis error rate. The smaller F means the current particle is better.

3. Coal mill modeling and condition monitoring

3.1. Main technical parameters of coal mills

The main components of medium-speed coal mill are as follows:
1) Motor-driven reduction gearbox: the reduction gearbox consists of planetary gears, which is directly coupled with the grinding bowl with appropriate reduction ratio to make the grinding bowl reach the required rotational speed.
2) Side body: forming air inlet around the grinding bowl and supporting the separator body, introducing hot air through the wind ring and upward along the periphery of the grinding bowl.
3) Grinding bowl: Raw coal is squeezed and ground into powder above the grinding bowl.
4) Impeller device, i.e. wind ring: mounted on the outer circle of the grinding bowl, it makes the hot air from the primary air chamber evenly distributed.
5) Spring loading: three separate spring loadings are located above the grinding bowl so that the grinding rollers can rotate freely when the raw coal fills the gap between the grinding auxiliary and the grinding bowl.
6) Separator body: It consists of separator body, guide liner, separator top cover equipped with folding door device and inner cone, and separator.
7) Outlet venturi and multi-outlet device: these components divide the coal dust and airflow into four strands of even hook.

The main technical parameters of the coal mill are shown in Table 1.

Table 1. The main technical parameters of the coal mill

Project	Unit	Technical specification	
(1) Type		HP863	HP1003
(2)Quantity	Table/Furnace	10	10
(3)Maximum output	t/h	42.5	70.5
(4) Design force	t/h	33.1	55.3
(5) Minimum force	t/h	12.325	20.1
(6) Fines(R90)	%	19.5	22
(7) Maximum air flow	t/h	75	105
(8) Maximum resistance	kPa	6	6
(9) Mill speed	r/min	42.6	35.7
(10) Wind ratio		1.95	1.90
(11) Seal wind/wind differential pressure	kPa	3	3
(12)Reduction mode	Spiral bevel gear plus planetary gear secondary drive		

The internal air dusting process of the coal mill is as follows:

The coal mill is used to grind the raw coal to a fineness of pulverized coal that can be burned efficiently in the furnace. The raw coal falls onto the rotating grinding bowl through the feed pipe and moves radially outward towards the grinding ring under the action of centrifugal force. As a result of the radial and circumferential movement, the coal passes under a grinding stick device that can rotate around the shaft. The grinding force generated by the spring-loaded device acts on the coal through the rotating grinding stick, causing the coal to form a coal bed under the grinding stick and to be ground into powder between the grinding ring and the grinding aid. During the grinding of the coal, the lighter particles are continuously bitten up from the grinding bowl by the hot air.

3.2. Numerical simulation process

3.2.1. Computational models. The coal mill is mapped on site to obtain the actual dimensions of the coal mill. A model of the coal mill was constructed based on the actual dimensions of the coal mill and the model was simplified for what was being studied. The model does not include the separator at the upper part of the coal mill. The model consists of the inlet primary air duct, primary air chamber, wind ring and the upper cylinder of the coal mill. The dimensions of the corresponding numerical simulation model of the coal mill are shown in Table 2.

Table 2. The size of the corresponding grinding machine numerical simulation model

Coal mill	Primary chamber		Air ring			Upper space		Coal funnel	
	Radius /m	Altitude /m	Width /m	Altitude /m	Angle of dip/°	Radius /m	Altitude /m	Top radius/m	Coal tube radius /m
HP863	1.52	1.0	0.055	0.15	50	1.52	2.5	0.95	0.35
HP1003	1.78	1.0	0.075	0.22	50	1.78	2.8	1.00	0.50

3.2.2. Grid division. The success of numerical simulation depends largely on the quality of the mesh. At present, there are two main methods of drawing meshes: structured meshes and unstructured meshes. Structured grids have the advantages of good generation quality, simple structure, and easy convergence, but have the disadvantages of narrower applicability and limited generation range. Unstructured grids have good adaptability to complex computational regions, so they have been developed rapidly, but there are drawbacks such as not easy to converge, long computation time, and high computational cost.

The meshing in this paper adopts a combination of two drawing methods. The structured grid is used for the wind ring location, and the unstructured grid is used for the primary air chamber and the upper cylinder space of the coal mill, and the sections are connected by interface, and the total number of grids is 2.6 million.

3.2.3. Boundary conditions. The primary air in the coal mill is considered as an ideal gas with constant end-flow flow. The inlet of the primary air duct is set as the mass inlet boundary condition, the outlet plane of the upper cylinder of the coal mill is the model outlet, which is set as the fully developed boundary condition, and the solid wall surfaces of the coal mill are all adiabatic conditions. In the actual heat transfer process, the extrinsic moisture wrapped around the coal powder and part of the vaporizable intrinsic moisture are first heated by the primary air and vaporized. Therefore, the cone-type injection surface is set in the model, and the coal dust and moisture are uniformly sprayed into the coal mill interior along the edge of the grinding bowl, so that the heat exchange process between the primary wind and coal dust is close to the actual situation.

Neglecting the stony coal emissions, the particle size of the pulverized coal particles was adopted as Rosin-Rammler distribution. The minimum particle size was 1 μm, the maximum particle size was 300 μm, and the average diameter was 70 μm. The distribution index was 1.62, and the initial temperature of the pulverized coal particles was 26℃. Density 1500 kg/m^3, specific heat capacity 1800 $J/kg \cdot K$. The temperature at which water begins to evaporate is set at 12°C and the boiling point at 100°C.

3.2.4. Simulation of working conditions. In order to better correspond to the coal mill temperature field measurement test in the field, the laboratory numerically simulated the two types of coal mills respectively based on the relevant parameters of coal types in the test program.

The HP863 coal mill simulated the case of raw coal with 12.23% volatile moisture. The primary air volume is 70t/h and the coal feed volume is 35t/h.

HP1003 coal mill simulated the case of raw coal volatile moisture 8.21%. The primary air volume is 100t/h and the coal volume is 50t/h. The coal mill outlet temperatures are 85°C, 95°C and 100°C respectively. The coal mill inlet primary air temperature is adjusted according to the coal mill outlet temperature. When calculating the iteration, the gas-phase field is first calculated to obtain a certain degree of convergence of the flow field. Then the solid-phase field is calculated until convergence, and the convergence criterion is that the residual difference of each calculation is less than 10^{-3}.

3.3. Common Failures and Condition Monitoring

3.3.1. Common Failures of Coal Mills. The coal mill faults simulated in this section are all set to occur at 40 min, including inlet coal break fault, outlet coal blockage fault and coal spontaneous combustion fault, the specific forms are shown below:

1) Coal mill inlet broken coal fault refers to the fault caused by the clogging of the coal drop pipe or the failure of the coal feeder, which leads to an abnormal reduction of the coal feeding quantity at the inlet of the mill or even no coal feeding. As the coal mill inlet coal breakage is more complicated, this paper only considers the raw coal gradually blocking the falling coal pipe. Coal mill inlet coal breakage has the following characteristics:

(1) Due to the reduction of coal in the mill, resulting in the coal mill current then decreased, and in severe cases, the current drops to no-load current.

(2) A decrease in the differential pressure between the inlet and outlet of the mill due to a decrease in resistance within the mill.

(3) As a result of a small amount of coal in the mill can not absorb the excessive heat of the primary wind, resulting in a rapid increase in the temperature of the coal mill outlet.

2) Coal mill clogging failure refers to the raw coal moisture is too large, wind coal ratio mismatch or too much coal and other reasons lead to a large amount of coal and coal dust inside the mill, can not be timely primary air into the furnace chamber combustion and the resulting failure. Due to the coal mill plugging is more complex, only consider the raw coal moisture is too large leading to coal mill plugging, coal mill plugging failure has the following characteristics:

(1) Due to the rise in resistance within the mill, the pressure of the wind-powder mixture at the outlet of the mill decreases, which in turn leads to an increase in the differential pressure between the mill and the inlet and outlet.

(2) As the moisture of coal powder increases, the temperature of the outlet wind powder mixture decreases.

(3) Due to the increase in the amount of internal coal, resulting in a slight increase in the mill current, with the aggravation of the coal plugging situation will lead to the internal coal mill is full of coal, the mill rollers can not continue to work, grinding failure, mill current drops sharply.

3) Coal mill coal spontaneous combustion failure refers to the mismatch of hot and cold air ratio, burning coal with high volatile matter or coal dust with flammable materials and other reasons, resulting in coal dust fire inside the coal mill and other failures. Due to the coal mill coal spontaneous combustion failure is more complex, only consider the coal spontaneous combustion due to the combustion of coal with high volatile matter. Coal mill coal spontaneous combustion failure has the following characteristics:

(1) Rapid increase in outlet temperature due to spontaneous combustion of coal dust in the mill.

(2) Due to the role of the coal mill control system itself, the hot air door opening is closed to zero, and the cold air door is fully open, the primary air flow is rapidly reduced, and then the differential pressure between the coal mill inlet and outlet is reduced.

3.3.2. Typical fault condition monitoring of coal mills. During actual operation in the field, the coal mill utilizes a closed-loop control strategy. Therefore, when a coal mill failure occurs, the control system will still maintain the output parameters of the coal mill at about the set value. Only when the equipment failure is so serious that the control system can not be adjusted, can the change in output data to reflect the degree of failure of the system. However, this often has a large lag.

The residual-based condition monitoring method characterizes the intrinsic physical relationship between the input and output parameters of the coal mill. Therefore, the typical coal mill fault data obtained from the previous simulation and the normal operation data are used to construct the residual sequence data of coal mill faults and combined with the statistical method to monitor the typical faults of the coal mill.

Assuming that the sequence of coal mill residuals obeys the normal distribution: $X \sim N_p\left(u,\Sigma\right)$, where p is the dimension of the residual sequence, then the operating state of the coal mill can be described by the Eq. (18) T^2 statistic:

$$T^2 = \left(X-u\right)^T \Sigma^{-1}\left(X-u\right) \tag{18}$$

where u is the residual series mean. Σ is the covariance matrix of the residual series, where the T^2 statistic obeys the distribution in equation (19):

$$T^2 \sim \frac{(n+1)(n-1)p}{n(n-p)}F(p,n-p) \tag{19}$$

where n is the number of sample points and F is the Fisher distribution.

The upper limit $T^2_{\max}$ of T^2 is determined according to equation (20):

$$T^2_{\max} \sim \frac{(n+1)(n-1)p}{n(n-p)}F_{1-\alpha}(p,n-p) \tag{20}$$

where α is the confidence level.

The coal mill condition monitoring using the T^2 statistic is divided into two sessions.

Session 1 includes:

1) Selecting n sets of fault residual data $\{X_i\}$ as training data, where $i=1,2,3,\ldots,n$ the mean and variance of the training data are calculated using Eqs. (21) and (22). Namely:

$$\overline{X} = \frac{1}{n}\sum_{i=1}^{n} X_i \tag{21}$$

$$S = \frac{1}{n-1}\sum_{i=1}^{n}\left(X_i-\overline{X}\right)^T\left(X_i-\overline{X}\right) \tag{22}$$

2) Set the value of confidence α and derive $T^2_{\max}$.

3) Calculate the T^2 statistic for each training data using equation (23). Namely:

$$T_i^2 = \left(X_i-\overline{X}\right)^T S^{-1}\left(X_i-\overline{X}\right) \tag{23}$$

4) Perform data screening to eliminate all data with T_i^2 greater than $T^2_{\max}$.

5) Repeat (1)~(4) until all data points satisfy T_i^2 is less than $T^2_{\max}$.

Session 2: Based on the $\overline{X}$ and S obtained in session 1, find T_i^2 of the measured data and compare it with $T^2_{\max}$. If T_i^2 is greater than $T^2_{\max}$, then the coal mill is considered to have failed.

4. Early warning of abnormal operating conditions of coal mills

4.1. *PSO-3DResNet-based anomaly monitoring algorithm*

In this subsection, the PSO-3DResNet model is used to compare the PSO-3DResNet model with the 3DResNet, SERNet, repVGG, and ResNeXt models in a comparison experiment using the blast furnace wind gap image dataset.

The image classification models for the comparison experiments include 3DResNet, SERNet, repVGG, and ResNeXt models, of which the 3DResNet model is a residual network model without particle swarm optimization. The SERNet model is a residual network model with unimproved channel attention. The repVGG model is an extension of VGG16. ResNeXt contains a main body network structure and a multi-branch network structure where each branch has the same structure.

4.1.1. Experimental parameterization. To avoid memory overflow, batch training is used to compare the PSO-3DResNet model with 3DResNet, SERNet, repVGG, and ResNeXt models in the training and validation sets, and the experiments are run on pycharm.

The experiments set the number of iteration rounds as 500, the loss function is selected as cross-entropy loss function, the optimization algorithm is stochastic gradient descent algorithm (SGD), and the settings of hyper-parameters batchsize and learning rate are experimented by group combination. Among them, batchsize is taken as 15, 30, 60, and learning rate is taken as 0.1, 0.01, 0.001, and there are 9 combinations.

At the same time, the dataset trained under different division methods fluctuates greatly, and the average results obtained by repeating the experiment several times can yield a good approximation of the generalization results. Therefore, the experiments use K-fold cross validation for parameter selection to improve the accuracy of model evaluation, determine the optimal parameter combinations, and ultimately use the saved model structure and parameters for the classification of anomalous states in blast furnace wind gap images.

The K value of K-fold cross-validation is set to 5, and the dataset is evenly divided into 5 parts, of which 4 parts are used as the training set and 1 part is used as the validation set. The experiment as a whole is to be run 5 times and the 5 validation results are averaged as the validation error of this model.

The optimal combination of parameters for each model is shown in Table 3, where the PSO-3DResNet model has a batchsize of 30, a learning rate of 0.1, and an average accuracy of 96.526%.

Table 3. The optimal parameter combination of each model

Model	batchsize	Learning rate	Average accuracy
PSO-3DResNet	30	0.1	96.526%
3DResNet	15	0.1	93.19%
SRENet	30	0.1	95.763%
repVGG	60	0.1	94.212%
ResNeXt	30	0.1	95.331%

4.1.2. Classification of Blast Furnace Air Opening Working Condition. The classification of blast furnace wind working state by each model is shown in Fig. 1. The PSO-3DResNet model has the best results in the slag hanging and coal breaking categories. The PSO-3DResNet model achieves the best classification accuracy in the classification of other categories except for wind rest.

Since the image features of the blast furnace in the slag-hanging and coal-break states are more easily captured than those of the other states, each model performs well in the feature extraction and classification of these two categories, with an accuracy of more than 97.5%. In addition, there are three similar categories of images in the collected image dataset of the blast furnace wind opening, which are material block, falling large block, and normal. For the model, the feature extraction and classification of these three types of images is difficult, but the accuracy rate can still reach more than 92%, achieving better classification results.

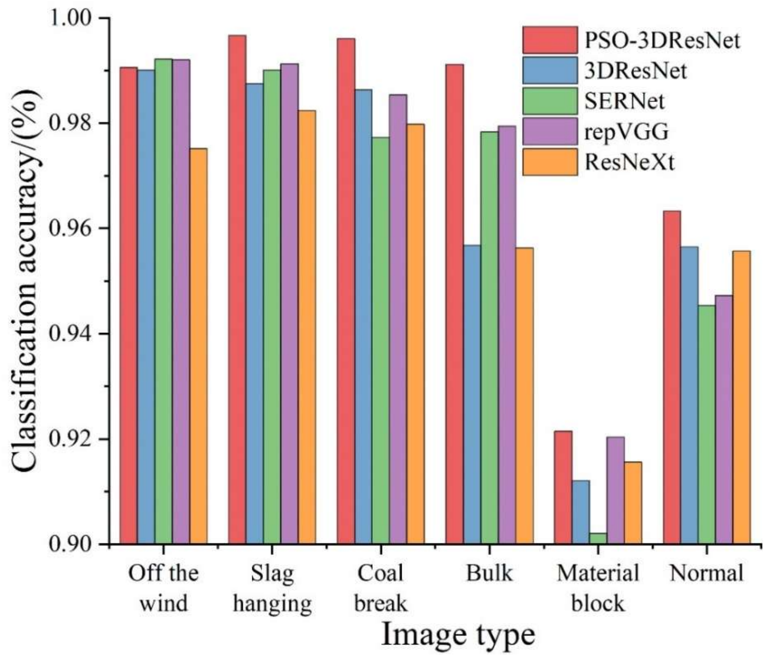

Figure 1. The classification of the working state of the blast furnace of various models

4.2. *Analysis of coal mill normal condition monitoring results*

By obtaining the reconstructed output of each input parameter under the normal operating state of the coal mill, the model has a better reconstruction effect when the coal mill is in the normal state. When the coal mill is in abnormal state, the reconstruction ability of the model decreases and the reconstruction error increases. The numerical simulation model of the coal mill established in the previous section and the historical operation data are used to verify the effectiveness of the proposed PSO-3DResNet model for monitoring the operation status of the coal mill.

The reconstruction results and relative errors of the differential pressure and outlet temperature of the coal mill are used as examples to analyze the effectiveness of the proposed model.The reconstruction values and relative error curves of the PSO-3DResNet model are shown in Fig. 2, and Figs. (a) to (d) are the reconstructed values of the differential pressure, the relative error of the differential pressure, the reconstructed values of the outlet temperature, and the relative error of the outlet temperature, respectively.

When the coal mill is in normal operation, the model reconstruction value and the actual measured value curve are very close to each other both numerically and morphologically. The relative error of the model is small, indicating that the PSO-3DResNet model is able to dig deeper into the nonlinear mapping relationship between the coal mill data and the operating state, and to fully learn the essential characteristics of the multivariate data, which can be crucial for the condition monitoring of the coal mill.

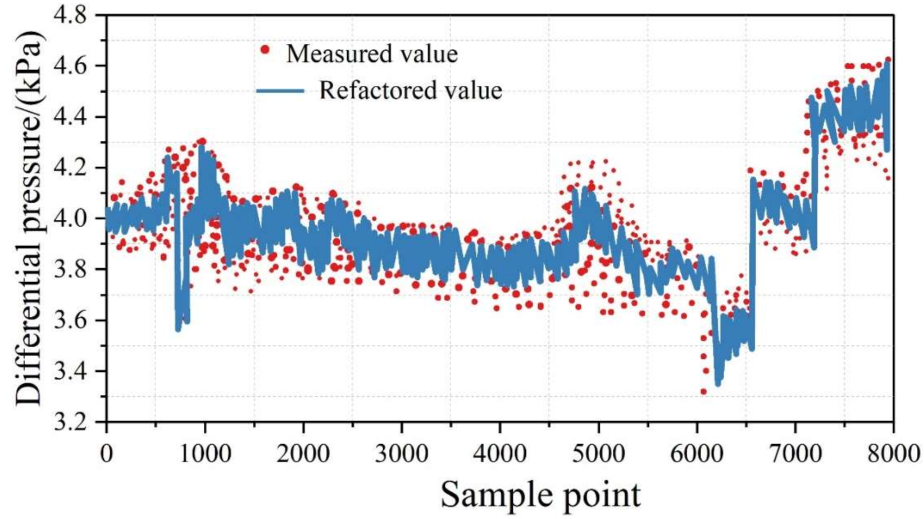

(a) Refactorings of differential pressure

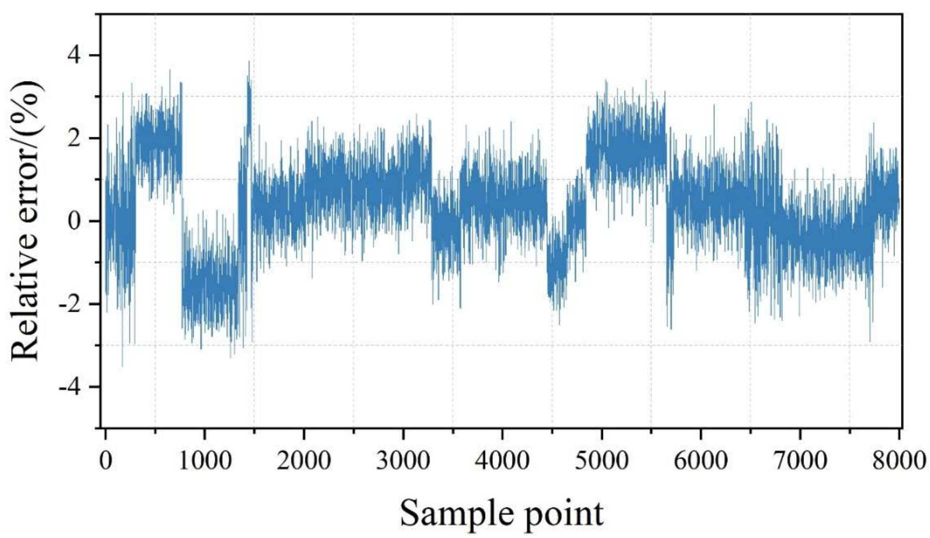

(b) Relative error of differential pressure

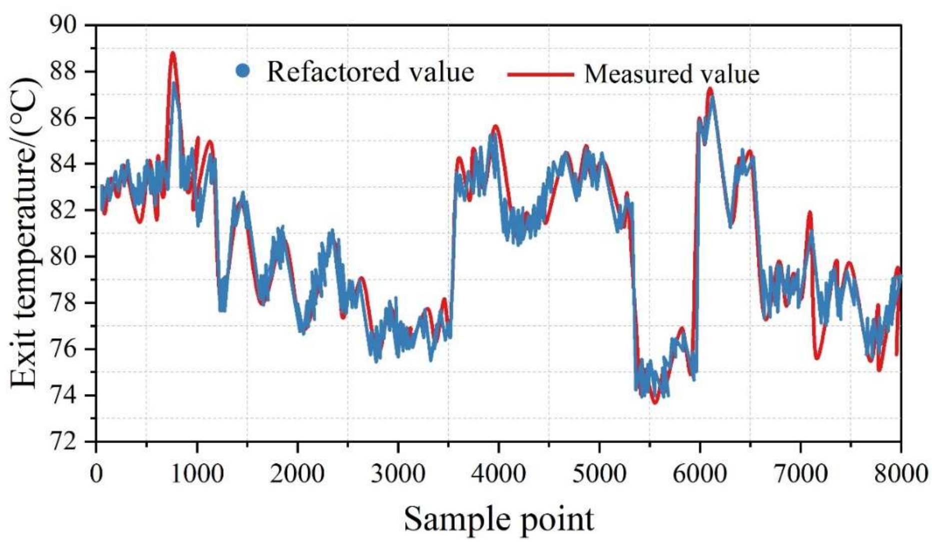

(c) The reconstruction value of the export temperature

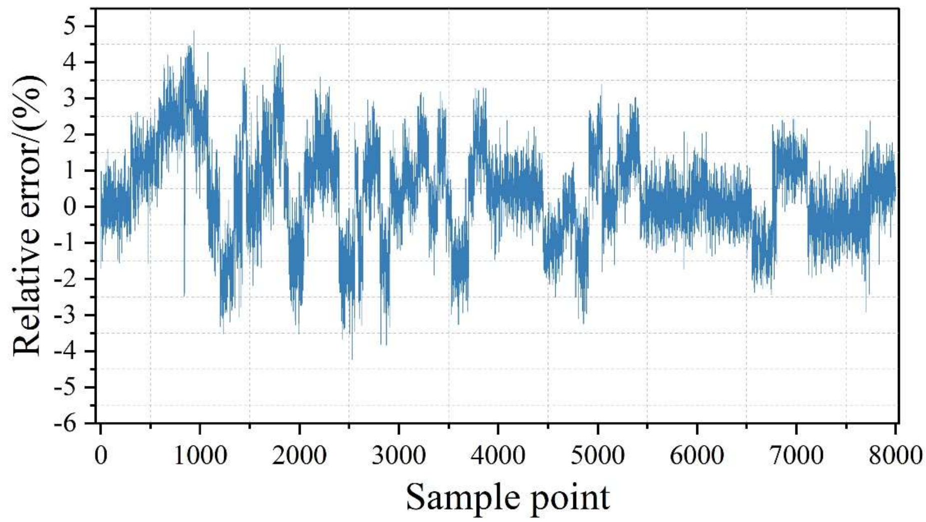

(d) Relative error of exit temperature

Fig. 2. The reconstruction value and relative error curve of the pthe 3dresnet model

When the coal mill is in normal operation, the one-dimensional condition monitoring indicators are obtained by calculating the Mahalanobis distance of the reconstructed residuals of the PSO-3DResNet model as shown in Fig. 3. The condition monitoring index fluctuates up and down within the range allowed by the threshold value and does not cross the pre-set threshold value. It indicates that the coal mill is in normal operation and no abnormality occurs, which is consistent with the actual operation status of the coal mill. It is verified that the established PSO-3DResNet model can monitor the operating status of the coal mill.

In actual production, the coal mill from the normal operating state transition to blockage failure state, usually in the transition process through a period of "critical blockage" state, at this time into the boiler the amount of pulverized coal will be lower than the amount of coal feed, resulting in a reduction in the unit's main steam pressure, load drop. If the "critical clogging" condition continues, it will eventually lead to a clogging abnormality in the coal mill.

There are three main reasons for the clogging of the coal mill:

1) The coal feeder feeds too much coal or the primary air volume at the inlet of the coal mill is too small, resulting in the accumulation of coal dust inside the coal mill, which can not be discharged in time.

2) Higher water content in the raw coal or lower wind temperature at the inlet of the coal mill leads to the inability of the coal mill to dry the coal powder sufficiently, which is also prone to cause blockage.

3) Poor grindability of raw coal or wear and tear of grinding parts can also lead to abnormal occurrence of clogging of raw coal inside the coal mill.

The test set data contains data on normal operating conditions and data on the occurrence of clogging abnormalities in the coal mill. According to the working mechanism of the coal mill, it can be seen that when the coal mill is clogged, its main state parameters will also change. The main performance is that with the reduction of coal feeding, the mill current will increase, the outlet temperature will decrease, and the differential pressure between the inlet and outlet of the coal mill will increase. Theoretically, the ratio of the coal mill current to the amount of coal fed will also gradually increase. The current of coal mill is the most sensitive index to the change of coal feed, and the strong correlation between coal feed and current of coal mill can be used to preliminarily judge the operation status of coal mill. Under normal operation, the rate of change of coal mill feeding quantity and coal mill current basically remains consistent, and will not be in a mismatch for a long time. If there is a long time mismatch between the coal feed quantity and mill current, it can be initially considered that there is an abnormal trend in the operating status of the coal mill.

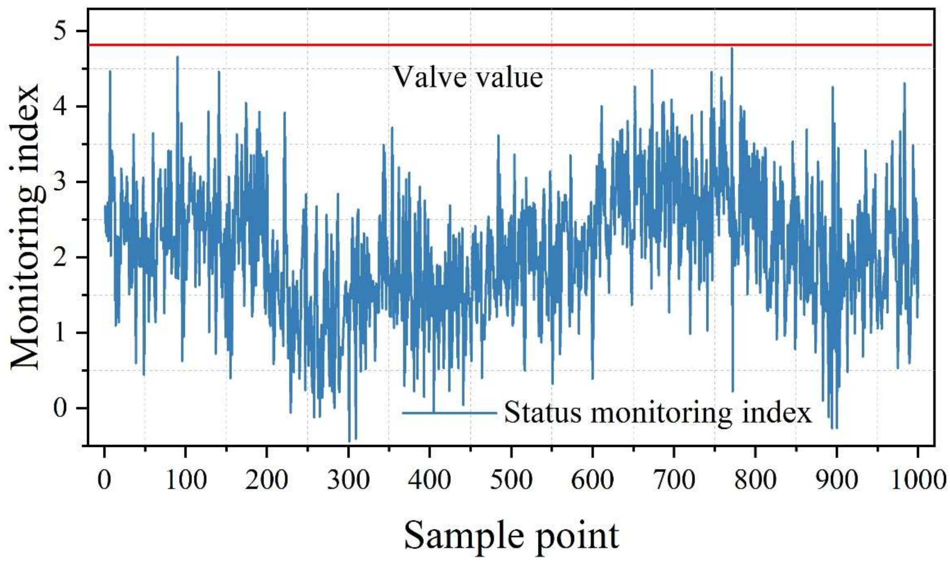

Fig. 3. Monitoring indicators under normal state of coal mill

4.3. Example of abnormal warning of coal mill operation status

In order to verify the feasibility and reliability of the PSO-3DResNet model for early warning of coal mill operating condition anomalies, the model was experimented with using historical coal mill current and outlet air temperature anomaly data. The data comes from a coal mill current and outlet air temperature anomaly that occurred on July 6, 2023. The data was obtained from the DCS system of the power plant with a fetch interval of 1 second. The obtained data are brought into the PSO-3DResNet model for calculation and estimation, and the residuals between the observed and estimated values are calculated.

The estimated results of the coal mill current anomalies and the residual values are shown in Fig. 4, and Figs. (a) and (b) show the estimated results of the current anomalies, and the current anomalies exponentially weighted average residuals, respectively. Figure (a) shows that the residual values always remain within [-16,3] and the residual curves show small fluctuations. Figure (b) shows that the current anomaly working condition index weighted average residuals remain within [-4,1].

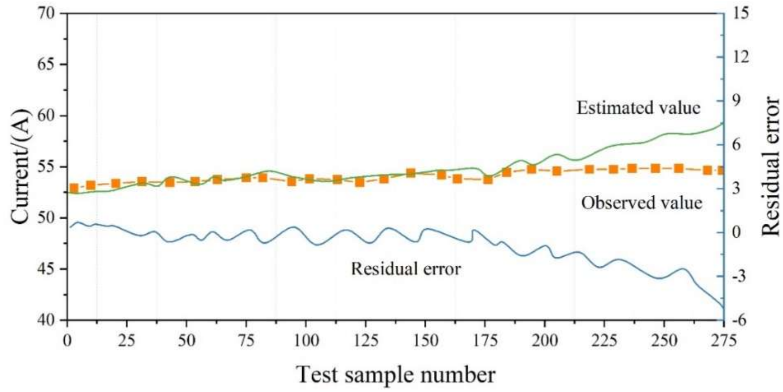

(a) Estimated result

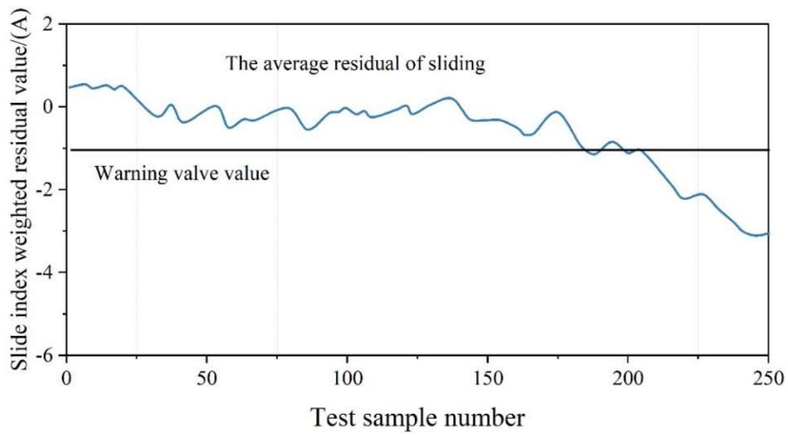

(b) Index weighted mean residual

Fig. 4. Estimated results of current abnormal conditions and residual errors

The coal mill outlet temperature anomaly working condition index and the index-weighted average residuals are shown in Fig. 5. Figures (a) and (b) show the export temperature anomaly working condition index and the weighted average residual of the export temperature working condition index, respectively. The weighted residual value of the sliding index of the outlet temperature working condition of the coal mill is in the interval of [-10,0].

During stable operating conditions, the sliding index weighted average residuals between the observed and estimated values of coal mill current and outlet temperature have been kept within the warning thresholds, and their fluctuation ranges are also good. However, when the operation of the coal mill is abnormal, the observed values and estimated values begin to have a large deviation, and the absolute value of the residuals of the sliding exponent weighted average soon breaks through the warning threshold and continues to increase, indicating that the fault problem is increasing.

The above analysis results can prove that the 3DResNet model based on particle swarm optimization can well capture the abnormal changes of the parameters in the operating state of the medium-speed coal mill and provide timely warning at the early stage of the abnormal operating state.

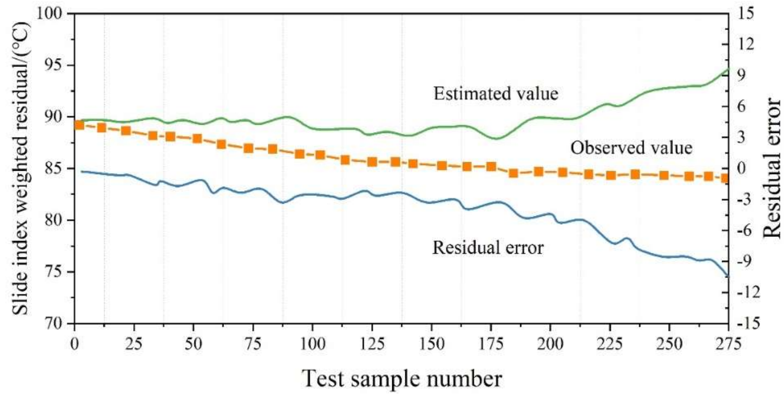

(a) Abnormal condition index

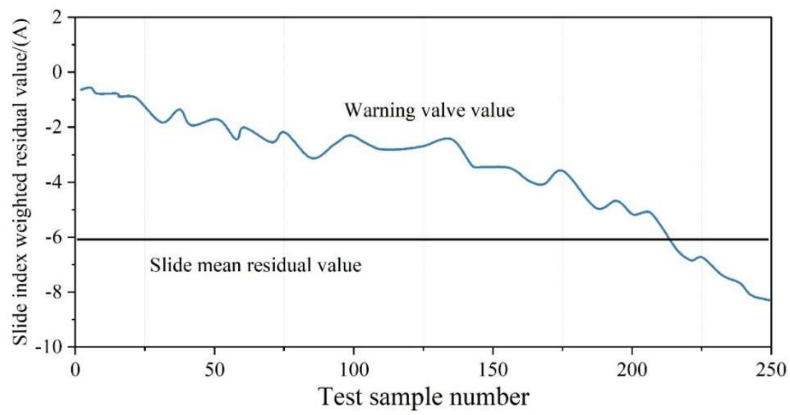

(b) Index weighted mean residual

Fig. 5. The export temperature abnormal condition index of the grinder

5. Conclusion

In this paper, particle swarm optimization 3DResNet network is used to construct a monitoring model for coal mill operation status. Analyze the parameter settings of the monitoring model, compare the classification accuracy of each model on the working state of blast furnace wind mouth, and monitor different states of coal mill operation.

Using the typical fault condition monitoring model of coal mill to compare the classification performance of each comparison model, the classification accuracy of PSO-3DResNet model for the six states of wind break, slag hanging, coal break, falling chunks, chunks of material, and normal is more than 92%.

The PSO-3DResNet model is used to analyze the reconstructed value of the differential pressure, the relative error of the differential pressure, the reconstructed value of the outlet temperature, and the relative error of the outlet temperature of the coal mill under normal state. Under the normal operation condition of the coal mill, the reconstructed value of the model is similar to the curve of the actual measured value, and the relative error is small.

Under the abnormal state of the coal mill, the PSO-3DResNet model calculates the weighted average residuals of the coal mill current abnormal condition index to remain in the range of [-4,1], and the weighted residual values of the sliding index of the outlet temperature condition are in the interval of [-10,0]. And when the observed values begin to show large deviations from the estimated values, the coal mill failure problem is in a state of increasing.

References

[1] Gao, Y., Zeng, D., & Liu, J. (2017). Modeling of a medium speed coal mill. Powder Technology, 318, 214-223.

[2] Hu, Y., Ping, B., Zeng, D., Niu, Y., & Gao, Y. (2020). Modeling of coal mill system used for fault simulation. Energies, 13(7), 1784.

[3] Weiming, Y., Yefa, H., Guoping, D., Kai, Y., Xuefei, C., & Xifei, C. (2023). Fault diagnosis of coal mills based on a dynamic model and deep belief network. Measurement Science and Technology, 34(12), 125052.

[4] Yin, W., Hu, Y., Ding, G., Xu, W., Feng, L., Chen, X., & Cao, X. (2024). Health indicator construction and application of coal mill based on the dynamic model. Structural Health Monitoring, 23(2), 686-700.

[5] He, K., Ren, X., Cheng, G., Wang, Y., Li, D., & Liu, H. (2021, December). Event monitoring of coal mill operation state based on acoustic fingerprint. In Second IYSF Academic Symposium on Artificial Intelligence and Computer Engineering (Vol. 12079, pp. 641-644). SPIE.

[6] Wang, W., Bai, X., & Liang, W. (2019, October). Optimization and transformation of 300MV units steel ball coal mill Pulverizing System. In IOP Conference Series: Materials Science and Engineering (Vol. 631, No. 2, p. 022072). IOP Publishing.

[7] Zhang, Z., Zhang, Y., Shen, W., & Lyu, X. (2023, June). Multi-objective Optimization of Coal Mill Outlet Temperature Control Using MPC. In 2023 9th International Symposium on System Security, Safety, and Reliability (ISSSR) (pp. 314-320). IEEE.

[8] Jie, D. (2021, August). Fault analysis and optimization technology of HP bowl type medium speed coal mill. In Journal of Physics: Conference Series (Vol. 2005, No. 1, p. 012217). IOP Publishing.

[9] Lu, H., Guo, X., Liu, Y., & Gong, X. (2015). Effect of particle size on flow mode and flow characteristics of pulverized coal. KONA Powder and Particle Journal, 32, 143-153.

[10] Pradeebha, P., Pappa, N., & Vasanthi, D. (2013). Modeling and control of coal mill. IFAC Proceedings Volumes, 46(32), 797-802.

[11] Krauze, O. (2023). Model and simulator of inlet air flow in grinding installation with electromagnetic mill. Scientific Reports, 13(1), 8281.

[12] Zhang, X., Winchester, N., & Zhang, X. (2017). The future of coal in China. Energy Policy, 110, 644-652.

[13] Lin, J., Fridley, D., Lu, H., Price, L., & Zhou, N. (2018). Has coal use peaked in China: Near-term trends in China's coal consumption. Energy policy, 123, 208-214.

[14] Hong, X., Xu, Z., & Zhang, Z. (2019). Abnormal condition monitoring and diagnosis for coal mills based on support vector regression. IEEE Access, 7, 170488-170499.

[15] Kurek, T., Wojdan, K., Nabagło, D., & Świrski, K. (2018). Detection of malfunctions and abnormal working conditions of a coal mill. In Thermal Power Plants-New Trends and Recent Developments. IntechOpen.

[16] Huang, C., Qu, S., Ke, Z., & Zheng, W. (2024). Dual fault warning method for coal mill based on Autoformer WaveBound. Reliability Engineering & System Safety, 245, 110030.

[17] Agrawal, V., Agrawal, S., Nag, S., Chakraborty, D., Panigrahi, B. K., & Subbarao, P. M. V. (2016, March). Application of K-NN regression for predicting coal mill related variables. In 2016 International Conference on Circuit, Power and Computing Technologies (ICCPCT) (pp. 1-9). IEEE.

[18] Wang, Y., Yu, J., Liang, H., Li, Q., Hu, P., & Wang, D. (2024). Modeling on rapid prediction and cause diagnosis of boiler combustion efficiency. Energy, 131848.

[19] Li, Y., Tian, L., Gao, Y., & Li, Y. (2019, November). Monitoring Model of Coal Mill in Power Plant Based on Big Data and BP Neural Network. In 2019 Chinese Automation Congress (CAC) (pp. 3451-3454). IEEE.

[20] Chao Wu,Shuo Yang,Donglai Jiao,Yixiang Chen,Jing Yang & Bo Huang. (2024). Estimation of daily XCO2 at 1 km resolution in China using a spatiotemporal ResNet model.. The Science of the total environment176171.

[21] Wenwen Zhang,Mingxuan Pan,Peng Wang,Jiao Xue,Xinghu Zhou,Wenke Sun... & Zhaopeng Shen. (2024). Comparative Analysis of XGB, CNN, and ResNet Models for Predicting Moisture Content in Porphyra yezoensis Using Near-Infrared Spectroscopy. Foods(19),3023-3023.

[22] Bo Sun,Peixi Peng,Guang Tan,Mingjun Pan,Luntong Li & Yonghong Tian. (2024). A fuzzy logic constrained particle swarm optimization algorithm for industrial design problems. Applied Soft Computing(PC),112456-112456.